LETTERS

Early human use of marine resources and pigment in South Africa during the Middle Pleistocene

Curtis W. Marean[1], Miryam Bar-Matthews[3], Jocelyn Bernatchez[2], Erich Fisher[4], Paul Goldberg[5], Andy I. R. Herries[6], Zenobia Jacobs[7], Antonieta Jerardino[8], Panagiotis Karkanas[9], Tom Minichillo[10], Peter J. Nilssen[11], Erin Thompson[1], Ian Watts[12] & Hope M. Williams[2]

Genetic and anatomical evidence suggests that *Homo sapiens* arose in Africa between 200 and 100 thousand years (kyr) ago[1,2], and recent evidence indicates symbolic behaviour may have appeared ~135–75 kyr ago[3,4]. From 195–130 kyr ago, the world was in a fluctuating but predominantly glacial stage (marine isotope stage MIS6)[5]; much of Africa was cooler and drier, and dated archaeological sites are rare[6,7]. Here we show that by ~164 kyr ago (±12 kyr) at Pinnacle Point (on the south coast of South Africa) humans expanded their diet to include marine resources, perhaps as a response to these harsh environmental conditions. The earliest previous evidence for human use of marine resources and coastal habitats was dated to ~125 kyr ago[8,9]. Coincident with this diet and habitat expansion is an early use and modification of pigment, probably for symbolic behaviour, as well as the production of bladelet stone tool technology, previously dated to post-70 kyr ago[10–12]. Shellfish may have been crucial to the survival of these early humans as they expanded their home ranges to include coastlines and followed the shifting position of the coast when sea level fluctuated over the length of MIS6.

The Middle Stone Age (MSA) was the technological phase (appearing as early as 280 kyr ago[13]) of the origins of modern humans. South Africa has provided a rich and important MSA archaeological record that mostly post-dates 120 kyr ago, but many of the excavated sites occur at elevations at which the MIS5e high sea stand (~+6 m above mean sea level at 123 kyr ago) would have washed out earlier deposits[14]. Co-occurring with an increase in the frequency of known coastal sites younger than 120 kyr is a burgeoning of material cultural complexity. In addition to the later appearance of bone tools[15] and beads[3], there is extensive evidence for systematic use of pigment by 120 kyr ago in South Africa[16]. Pigments near this age, or older, are patchily distributed outside South Africa; for example, in Israel some are dated to 92 kyr ago[17], at Twin Rivers in Zambia they are dated to between 141 and >400 kyr ago[18], and 'red ochres' from the Kapthurin Formation in Kenya are dated to >285 kyr ago[7].

Site PP13B (S34° 12′ 44″ E22° 05′ 37″) is a sea cave overlooking the Indian Ocean in the quartzitic coastal cliffs at Pinnacle Point near Mossel Bay (South Africa). It escaped the MIS5e high sea stand by virtue of its elevation (+15 m above mean sea level, see Supplementary Information and Video). On the north and south walls of the cave is a variably cemented MSA deposit (called the LC-MSA), whereas the floor is covered by a mostly uncemented MSA deposit (Fig. 1)[19]. We excavated three areas in the cave, but our focus here is on the LC-MSA deposits, which are the oldest sediments with significant anthropogenic input.

We recognize the following stratigraphic sequence in the LC-MSA deposits, from bottom to top. The LC-MSA Lower has a weighted mean optically stimulated luminescence (OSL) age of 164 ± 12 kyr (Table 1 and Supplementary Information, for all ages that we present). It is a sandy deposit, the least cemented of all, with multiple lenses of burnt carbonaceous material; micromorphology and frequency-dependent magnetic susceptibility analysis show that some of these are *in situ* combustion features. Lithics and faunal remains are abundant throughout, but are concentrated in burnt lenses. The plotted finds are inclined mostly between 0 and 15°, with few dramatic changes that would indicate intrusions or disturbances (Supplementary Information). The LC-MSA Middle (weighted-mean OSL age of 132 ± 12 kyr) is mostly ash, has multiple lenses of dark organic material that micromorphology shows are *in situ* hearths, and has a plotted find density less than the LC-MSA Lower. The LC-MSA Upper is a heavily cemented zone with three sub-units: (1) a lower hard sandy and silty layer containing reworked ashes that directly contacts and transitions into the richer anthropogenic deposits of the LC-MSA Middle; (2) a layer of shellfish stratified within an aeolian dune with a weighted mean OSL age of 120 ± 7 kyr; and (3) a dune that sealed the cave, and which has a weighted mean OSL age of 90 ± 6 kyr. Capping the deposit, the LC-MSA Flowstone is a 5-cm-thick laminated flowstone with a rough and wavy microscopically sharp boundary with the underlying LC-MSA Upper. Six uranium series (U-series) ages on separate laminae range from 39 to 92 kyr (Table 1), providing high resolution minimum ages for everything below. Several forms of evidence suggest partial closure of the cave from 39 to 92 kyr ago (Supplementary Information).

The LC-MSA Lower falls within MIS6, during which sea level was lower than today. We have developed a three-dimensional Geographical Information Systems (GIS) model (Supplementary Video and Information) that joins offshore bathymetry to a relative sea level curve[20] and models the coastline at 1.5-kyr increments for the last 400 kyr. Studies of modern and recent archaeological shellfish transport show that foragers rarely transport shell over more than 5–10 km[9,21]. Our model shows that the coastline was within that distance during MIS6 only at 167 kyr ago—a result concordant with the OSL ages.

The flaked-stone-artefact assemblage ($n = 1836$) is quartzite dominated (78%) and includes Levallois technology, often considered characteristic of the MSA[22], as well as bladelet technology, which is more typical of much later periods[10,11](Fig. 2). The blades form a continuous size distribution of widths from large blades to bladelets. Bladelets here conform to the formal definition of blades less than

[1]Institute of Human Origins, [2]School of Human Evolution and Social Change, PO Box 872402, Arizona State University, Tempe, Arizona 85287-2402, USA. [3]Geological Survey of Israel, 30 Malchei Israel Street, Jerusalem 95501, Israel. [4]Department of Anthropology, University of Florida, Gainesville, Florida 32611, USA. [5]Department of Archaeology, Boston University, 675 Commonwealth Avenue, Boston, Massachusetts 02215, USA. [6]Human Origins Group, School of Medical Sciences, The University of New South Wales, Sydney NSW 2052, Australia. [7]School of Earth and Environmental Sciences, University of Wollongong, Wollongong, 2522, Australia. [8]Department of Archaeology, University of Cape Town, Rondebosch 7701, South Africa. [9]Ephoreia of Palaeoanthropology-Speleology, Ministry of Culture, Ardittou 34b, Athens 11636, Greece. [10]Department of Anthropology, University of Washington, Box 353100, Seattle, Washington 98195-3100, USA. [11]Archaeology Division, Iziko-South African Museum, PO Box 61, Cape Town 8000, South Africa. [12]58 Eastdown House, Downs Estate, Amhurst Road, London E8 2AT, United Kingdom.

10 mm in width. Thirty-five plotted finds meet this definition and an additional 29 bladelets or bladelet fragments were recovered from the 3-mm screens (Supplementary Information). Bladelet technology is a significant component of the lithic assemblage: for example, in the LC-MSA Lower the total number of true bladelets ($n = 64$) exceeds the total number of Levallois products ($n = 47$).

There are 57 pigment pieces (93.4 g total) and most are from the LC-MSA Lower. Forty-six are iron-rich fine-grained sedimentary materials, and most have a pinkish-brown or reddish-brown surface colour. Streak colour (Natural Colour System) shows the majority ($n = 31$) as intermediate reddish-brown, followed by saturated reddish-brown ($n = 10$), and saturated very red ($n = 7$, high chroma values and ≥75% redness). All can be classified as 'red ochre'. Ten pieces were definitely used (eight ground and two scraped) and two pieces were probably used (both ground). Most ground pieces are moderately to intensively ground on one principal surface (Fig. 2). Saturated very-red values are disproportionately represented among used pieces, suggesting preferential use of the reddest, most chromatic ochre (Supplementary Information).

Fifteen categories of marine invertebrates are so far documented in the PP13B deposits (Table 2): four categories to species level (*Perna perna*, *Choromytilus meridionalis*, *Scutellastra argenvillei* and *Turbo*

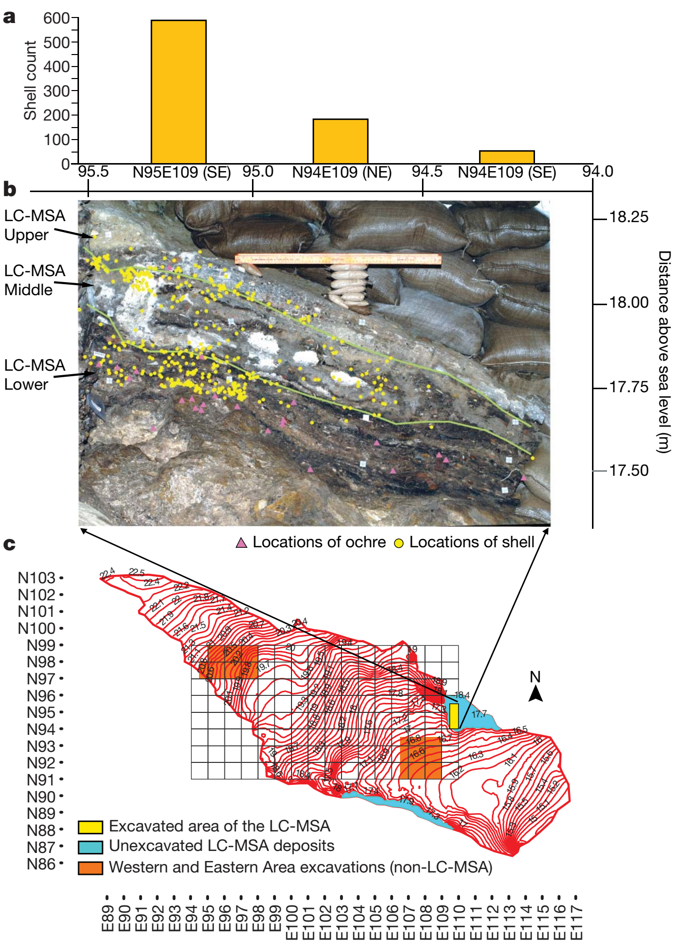

Figure 1 | Contour map of PP13B, photograph of the LC-MSA eastern section, and the frequency of shellfish and ochre. a, The number of shellfish per 50 cm × 50 cm excavated quadrant (NE, north-east quadrant, SE, south-east quadrant; N95E109, 95 metres north and 109 metres east of the zero point; for explanation of MAP grid space see Methods) for all layers north to south. **b**, A geo-referenced section photograph of the eastern section with plotted ochre and shellfish on the photograph (see Supplementary Information for an un-geo-referenced version), and the main divisions of the layers indicated. **c**, A contour map of 13B showing the location of the LC-MSA deposits and the positions of the excavations within the MAP grid.

Table 1 | Radiometric ages from the LC-MSA at PP13B

U-series ages for the LC-MSA flowstone

Sample number	[U] (p.p.m.)	$^{234}U/^{238}U$	$^{230}Th/^{232}Th$	Uncorrected age (kyr)	Corrected age (kyr)	±2σ (kyr)
32204	1.2	2.58712	186	39.1	39.1	0.4
32203	0.06	2.47122	66	45.9	45.5	0.4
32202	0.97	2.39069	23.2	47.4	46.1	1.3
32200	0.495	1.84941	46.3	75	74.03	0.8
32201	0.36	2.39069	46	81.5	80.5	1.4
32205	0.79	2.05105	42.2	92.7	91.6	1

Optically stimulated luminescence ages on the LC-MSA sediments

Sample number	Stratigraphic position	Age (kyr)	±2σ (kyr)
46447	LC-MSA Upper (upper dune)	88.3	10.0
111400	LC-MSA Upper (upper dune)	89.3	8.2
46467	LC-MSA Upper (lower dune)	119.0	8.8
20720	LC-MSA Upper (lower dune)	121.3	8.4
111401	LC-MSA Upper (lower dune)	116.7	10.6
111402	LC-MSA Middle	135.2	12.8
111403	LC-MSA Lower	161.9	15.2
20721	LC-MSA Lower	167.7	18.2
111406	LC-MSA South Profile (lower)	161.7	17.0

Ages are ordered stratigraphically from top to bottom.

sarmaticus), five to genus level (*Donax* spp., *Helcion* sp., *Oxystele* spp., *Nodilittorina* spp., *Burnupena* spp.), three to Family level (Mytilidae, Patellidae and Turritellidae), one to Subphylum (shore barnacle, Crustacea), and two to only molluscs (whelks and chitons), to which, respectively, many families and an entire class belong. *P. perna* (brown mussel) is dominant, followed by *T. sarmaticus* (giant periwinkle), limpets (*S. argenvillei* and Patellidae) and small numbers of whelks. Brown mussels are the overwhelmingly dominant species in the LC-MSA Upper. On the basis of current habitats[23], the vast majority of shellfish were collected from exposed to moderate rocky shores and from tidal pools, easily achieved during daily low tides and/or monthly spring low tides. The whale barnacle fragment is tentatively identified as *Coronula diadema*[24], and suggests scavenging of beached whale blubber and skin with attached barnacles[25].

For millions of years, hominin diet was restricted to terrestrial plants and animals. The expansion to shellfish is one of the last

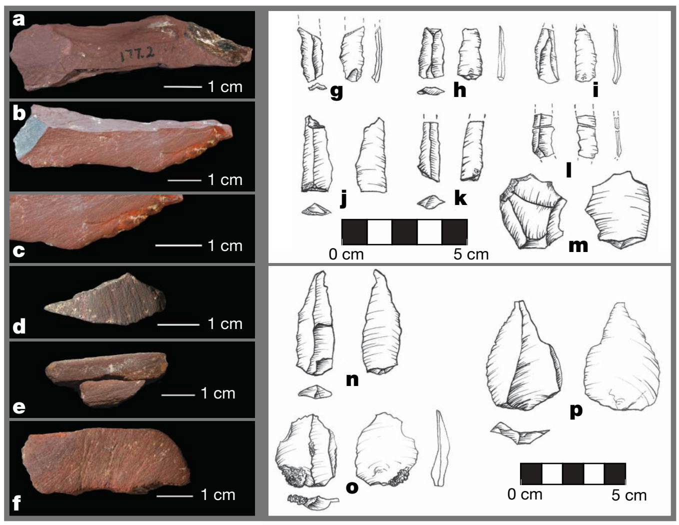

Figure 2 | Ochre and lithics from the LC-MSA Lower. a–c, Specimen 177.2 (moderately ground shale, moderately haematized, 17.1 g, NCS 3355 Y70R) three views: **a**, flaked surface. **b**, ground surface. **c**, close-up of ground surface. **d**, Specimen 79092 (ground fragment, haematite, 6 g, NCS 6727 Y75R). **e**, Specimens 81614 and 81681 (two conjoining ground fragments, siltstone, 2 g, NCS 3162 Y60R). **f**, Specimen 81770 (Intensively ground fragment, coarse siltstone, moderately haematized, 10.1g., NCS 3257 Y80R). **g–i**, Quartzite bladelets. **j**, Quartzite small blade. **k**, Quartzite bladelet. **l**, Quartzite bladelet fragments, refit. **m**, Quartzite core rejuvenation flake. **n**, Quartzite Levallois blade. **o**, Silcrete Levallois flake. **p**, Quartzite Levallois point.

Table 2 | The MNI and weight of shellfish in the LC-MSA layers

	LC-MSA Lower		LC-MSA Middle		LC-MSA Upper	
Species collected as food	MNI	Weight (g)	MNI	Weight (g)	MNI	Weight (g)
Mollusca						
Perna perna	14	118.5	39	310.0	20	157.8
Choromytilus meridionalis	1	2.9	1	3.1	0	0.0
Mytilidae	1	2.0	1	7.6	0	0.0
Donax spp.	1	1.1	0	0.0	0	0.0
Scutellastra argenvillei	0	0.0	1	5.1	0	0.0
Patellidae	1	5.8	5	27.0	1	0.1
Oxystele spp.	1	0.1	0	0.0	0	0.0
Turbo sarmaticus	1	9.4	4	30.7	0	0.0
Burnupena spp.	1	0.2	1	0.0	1	0.1
Whelk	1	0.8	1	1.9	0	0.0
Chiton	1	0.7	1	0.2	0	0.0
Epibionts or brought in incidentally						
Mollusca						
Turritellidae	0	0	1	<0.1	0	0
Helcion sp.	1	<0.1	1	<0.1	0	0
Nodilittorina spp.	1	0.1	4	0.3	1	0.2
Crustacea						
Cirripedia						
Shore barnacle	0	0	1	0.4	1	0.8
Coronula spp. (whale barnacle)	1	1.1	0	0	0	0

MNI, minimum number of individuals.

additions of a new class of food to the human diet before the introduction of domesticates at the end of the Pleistocene. Coastlines have few resources to attract hunter-gatherers if their diets do not include shellfish and/or fish. Once they do, coastlines become attractive for settlement and movement. It has been argued that shellfish exploitation was crucial to a potential early coastal route of modern humans out of Africa via the Red Sea coast[8], and marine adaptations made possible an early migration to Australia/New Guinea along a coastal corridor[26,27]. Our results show that the coastal adaptation was present in South Africa long before the postulated dates for these migrations (after 120 kyr ago). Shellfish may have been a critical food source to the survival of human populations when they were faced with depressed terrestrial productivity during glacial stages such as MIS6, a time when much of southern Africa was more arid[28] and populations were isolated and perhaps concentrated on now-submerged coastal platforms.

Shellfish can be a predictable food resource for humans[9] with substantial nutritional benefits[29]. Shellfish collecting is often associated with hunter-gatherer economic and social systems with greater complexity and reduced mobility[9], which are themselves excellent contexts for stimulating symbolic expression through material culture. The PP13B ochre sample has all the hallmarks of pigment for body-painting and perhaps colouring of other organic surfaces, and thus joins a patchy sample of Middle Pleistocene evidence for pigment use. By 164 kyr ago, there is preferential processing of the reddest pigments, as is present in more recent sites[16], showing the same pattern of pigment exploitation 40 kyr before its apparent fluorescence post 120 kyr ago. We have identified the earliest appearance of a dietary, technological and cultural package that included coastal occupation, bladelet technology, pigment use and dietary expansion to marine shellfish, and is dated to a time close to the biological emergence of modern humans.

METHODS SUMMARY

Owing to the small amount of preserved LC-MSA sediment, we conducted a limited excavation of a 1.5-m N–S section. We excavated within 50 cm × 50 cm quadrants within squares, named by their bearing: NE, NW, SE and SW. Excavations followed natural stratigraphic units (layers, features, and so on), and thus square-quadrant stratigraphic unit provenance designation is the minimum assigned to any find. Sediment volumes were measured during excavation, and bulk samples of sediment were taken from every unique stratigraphic unit. All observed finds were plotted directly to Total Station in three dimensions, whereas the rest were captured by nested 10-mm→3-mm→1.5-mm wet-sieving. Screened materials were dried, packed in plastic bags and transported to the field laboratory. All plotted finds were labelled with their specimen number in black India ink. Finds were then sorted in the laboratory and provided to the appropriate specialist for analysis (lithics, ochre and shellfish; see Author Contributions). Inclinations of finds were calculated from two shots on opposite ends of the finds. Lithics were analysed by a combination of typological, technological and metrical variables from a database of all plotted finds, and those from the 10-mm mesh screen. Ochre was studied under a 10–40× zoom microscope, and streak properties were ascertained by the production of a streak across white porcelain plates. Shellfish were identified by comparison to known modern specimens. The backgrounds of all photographic images of artefacts in Fig. 2 were removed. No portion of any artefact image was retouched or otherwise edited. Stratigraphic interpretations are derived from a combination of field-based macro-stratigraphic observations, computer analysis of mapped stratigraphic units, analyses of plotted find distributions, and micromorphology. Dating of the sediments is accomplished by OSL and U-series techniques.

Full Methods and any associated references are available in the online version of the paper at www.nature.com/nature.

Received 21 May; accepted 28 August 2007.

1. Ingman, M., Kaessmann, H., Paabo, S. & Gyllensten, U. Mitochondrial genome variation and the origin of modern humans. *Nature* **408,** 708–713 (2000).
2. McDougall, I., Brown, F. H. & Fleagle, J. G. Stratigraphic placement and age of modern humans from Kibish, Ethiopia. *Nature* **433,** 733–736 (2005).
3. Henshilwood, C., d'Errico, F., Vanhaeren, M., van Niekerk, K. & Jacobs, Z. Middle Stone Age shell beads from South Africa. *Science* **304,** 404 (2004).
4. Vanhaeren, M. *et al.* Middle Paleolithic shell beads in Israel and Algeria. *Science* **312,** 1785–1788 (2006).
5. Petit, J. R. *et al.* Climate and atmospheric history of the past 420,000 years from the Vostok ice core, Antarctica. *Nature* **399,** 429–436 (1999).
6. Marean, C. W. & Assefa, Z. in *African Archaeology* (ed. Stahl, A. B.) 93–129 (Blackwell, New York, 2005).
7. McBrearty, S. & Brooks, A. S. The revolution that wasn't: a new interpretation of the origin of modern human behavior. *J. Hum. Evol.* **39,** 453–563 (2000).
8. Walter, R. C. *et al.* Early human occupation of the Red Sea coast of Eritrea during the last interglacial. *Nature* **405,** 65–69 (2000).
9. Erlandson, J. M. The Archaeology of Aquatic Adaptations: Paradigms for a New Millennium. *J. Archaeol. Res.* **9,** 287–350 (2001).
10. Ambrose, S. H. Small things remembered: origins of early microlithic industries in sub-saharan Africa. *Archaeol. Pap. Am. Anthropol. Assoc.* **12,** 9–29 (2002).
11. Soriano, S., Villa, P. & Wadley, L. Blade technology and tool forms in the Middle Stone Age of South Africa: the Howiesons Poort and post-Howiesons Poort at Rose Cottage Cave. *J. Archaeol. Sci.* **34,** 681–703 (2007).
12. Villa, P., Delagnes, A. & Wadley, L. A late Middle Stone Age artifact assemblage from Sibudu (KwaZulu-Natal): comparisons with the European Middle Paleolithic. *J. Archaeol Sci.* **32,** 399–422 (2005).
13. Tryon, C. A. & McBrearty, S. Tephrostratigraphy and the Acheulian to Middle Stone Age transition in the Kapthurin Formation, Kenya. *J. Hum. Evol.* **42,** 211–236 (2002).
14. Hendey, Q. B. & Volman, T. P. Last interglacial sea levels and coastal caves in the Cape Province, South Africa. *Quat. Res.* **2,** 189–198 (1986).
15. Henshilwood, C. S., D'Errico, F., Marean, C. W., Milo, R. G. & Yates, R. J. An early bone tool industry from the Middle Stone Age, Blombos Cave, South Africa: implications for the origins of modern human behaviour, symbolism and language. *J. Hum. Evol.* **41,** 631–678 (2001).
16. Watts, I. Ochre in the Middle Stone Age of southern Africa: Ritualized display or hide preservative? *S. Afr. Archaeol. Bull.* **57,** 1–14 (2002).
17. Hovers, E. *et al.* An early case of color symbolism. *Curr. Anthropol.* **44,** 491–522 (2003).
18. Barham, L. S. Systematic pigment use in the Middle Pleistocene of South-Central Africa. *Curr. Anthropol.* **43,** 181–190 (2002).
19. Marean, C. W., Nilssen, P. J., Brown, K., Jerardino, A. & Stynder, D. Paleoanthropological investigations of Middle Stone Age sites at Pinnacle Point, Mossel Bay (South Africa): Archaeology and hominid remains from the 2000 Field Season. *Paleoanthropology* **2,** 14–83 (2004).
20. Waelbroeck, C. *et al.* Sea-level and deep water temperature changes derived from benthic foraminifera isotopic records. *Quat. Sci. Rev.* **21,** 295–305 (2002).
21. Bigalke, E. H. The exploitation of shellfish by coastal tribesmen of the Transkei. *Ann. Cape Prov. Mus. Nat. Hist.* **9,** 159–175 (1973).
22. Tryon, C. A., McBrearty, S. & Texier, P. J. Levallois lithic technology from the Kapthurin Formation, Kenya: Acheulian Origin and Middle Stone Age Diversity. *Afr. Archaeol. Rev.* **22,** 199–229 (2005).
23. Branch, G. *Two Oceans: A Guide to the Marine Life of Southern Africa* (D. Philip, Cape Town, 1994).

24. Newman, W. A. & Ross, A. Antarctic Cirripedia: Monographic Account Based on Specimens Collected Chiefly Under the United States Antarctic Research Program, 1962–1965. *Am. Geophys. Union. Antarct. Res. Ser.* **14,** 1–257 (1971).
25. Jerardino, A. & Parkington, J. New evidence for whales on archaeological sites in the south-western Cape. *S. Afr. J. Sci.* **89,** 6–7 (1993).
26. Kingdon, J. *Self-made man and his undoing* (Simon and Schuster, London, 1993).
27. Bulbeck, D. Where River Meets Sea: A Parsimonious Model for *Homo sapiens* Colonization of the Indian Ocean Rim and Sahul. *Curr. Anthropol.* **48,** 315–321 (2007).
28. Deacon, J. & Lancaster, N. *Late Quaternary Paleoenvironments of Southern Africa* (Clarendon Press, Oxford, 1988).
29. Broadhurst, C. L. *et al.* Brain-specific lipids from marine, lacustrine, or terrestrial food resources: potential impact on early African *Homo sapiens*. *Comp. Biochem. Phys. B.* **131,** 653–673 (2002).

Supplementary Information is linked to the online version of the paper at www.nature.com/nature.

Acknowledgements We thank the ISSR staff at ASU, the MAP staff for their assistance, the Dias Museum for field facilities, SAHRA and HWC for permits, and Waelbroeck for helping with sea level data. This research was funded by grants from the National Science Foundation (to C.W.M.) and the Hyde Family Foundation (to C.W.M.).

Author Contributions C.W.M. directed the excavations and is the project principal investigator. Authors made contributions in the following areas: M.B.-M., U-series dating; J.B., analysis of orientation and dip; E.F., three-dimensional GIS; P.G. and P.K., micromorphology and geology; A.I.R.H., geology and sediment magnetics; Z.J., OSL dating; A.J., shell analysis; T.M., E.T. and H.M.W., lithics; P.J.N., co-direction of the excavations; and I.W., ochre. All authors discussed the results and commented on the manuscript.

Author Information Reprints and permissions information is available at www.nature.com/reprints. Correspondence and requests for materials should be addressed to C.W.M. (curtis.marean@asu.edu).

METHODS

Excavation methods. Site PP13B was excavated within an arbitrary three-dimensional coordinate system (grid) called the MAP grid. All horizontal coordinates reported in this paper are in that grid space. It is tied to the South African National Coordinate Reference System, and our elevation measurements are in orthometric height above sea level as defined by that coordinate system. Our horizontal coordinates can be transformed to the South African grid using a two-dimensional conformal coordinate transformation, and from there to latitude and longitude following the Gauss Kruger Conform Projection using the Hartebeesthoek 1994 datum used by South Africa. In the MAP coordinate system, a 1 m square is named by the planar coordinates of its south-west corner. Published descriptions of our excavation methods are available[30,31].

Photography methods. The incorrect light settings of the camera for the image in Fig. 2b were corrected using Nikon Capture Editor 4 White Balance, with the camera white balance reset to 'daylight'. This correction was applied to the entire image. Figure 2c is a cropped higher resolution image of the whole artefact shown in Fig. 2b.

Much of the section photography presented here is geo-referenced to the MAP grid, unless otherwise indicated. This is accomplished in the following way. Targets are attached to the section approximately every 50 cm and these are shot to the Total Station. The photographs are then brought into ESRI ArcGIS and rectified (rotated and stretched) to the grid using those targets and their coordinates. This process creates a photograph that is true to elevation and one dimension of grid space to within several centimetres of its true geometric space, allowing one to plot on it finds that have been shot to the Total Station. There is a slight degradation of the image during the rectification process. For this reason, we have provided unedited versions of the two stratigraphic photographs (Supplementary Figs 1 and 2).

The micromorphology photographs (Supplementary Figs 3 and 4) were taken with a Zeiss Axioplan 40 POL polarizing microscope and an attached digital camera (Canon Powershot G5). A microscope $\times$12.5 magnification was used and a $\times$4 camera zoom. Digital image settings were auto-adjusted (for exposure, shadows, brightness and contrast) with Photoshop CS2. This adjustment was made uniformly to the entire image. No portion of the photographs was retouched or otherwise edited.

Lithic analysis methods. In the laboratory, the plotted and 10-mm screened materials were not washed. Each complete and fragmentary artefact was measured in standard multiple dimensions with a large number of traits recorded in a relational database. A basic shape typology and Geneste's[32] technological typology was recorded. All cores were recorded using the MSA typology of Volman[33] and the Geneste technological typology. Raw materials were recorded on the basis of geologic classes, which were easy to visually discriminate (only 0.2%, $N = 4$ unidentified/other).

Sea level GIS model method. The multidimensional GIS databases discussed in the text and featured within the Supplementary Video 1 were created using ESRI ArcScene and ArcGlobe 9.2. ESRI ArcScene was used primarily to model site-based archaeological and geological features within PP13B. The PP13B cave model represents a collection of more than 800 points shot along the floor and walls of the cave with a reflectorless Total Station. These points were then used to create a TIN model with Raindrop Geomagic software. The LC-MSA stratigraphic units visible in the model are a combination of 2.5-dimensional polygons representing the upper and lower surfaces of each unit and multipatch polygon convex hulls.

ESRI ArcGlobe was used for regional sea level modelling throughout the Pinnacle Point/Mossel Bay area. Base terrestrial elevations are a combination of regional SRTM 90 m digital elevation data and 1 m light detection and ranging (LIDAR) data around Pinnacle Point. The Pinnacle Point cliff face is a TIN model created from Total Station point survey data (over 30,000 shots) using Raindrop Geomagic. Additional imagery within the database includes 30 m resolution Landsat ETM+ images (Regional) and sub-orbital 1 m aerial photography (Pinnacle Point). The bathymetric data are a combination of high-resolution 1 m side-scanning sound navigation and ranging (SONAR) around Pinnacle Point and hand-digitization from published regional bathymetry maps. Sea level data were created by clipping the bathymetry elevation model to the listed depths below current relative sea level[34] and then converting the data into *z*-aware 3D polygons. Tabular output of this model is presented in Supplementary Table 1.

U-series dating methods. Six flowstone samples were collected from the flowstone capping the LC-MSA by chipping with a hammer from the horizontal extent of the *in situ* flowstone. The entire flowstone as well as each sample was mapped by Total Station. The flowstone was then cored to produce the micromorphology sample. Details of the U-series laboratory methods are presented in Supplementary Information.

OSL dating methods. Nine sediment samples were collected from the LC-MSA in the North Area of Cave 13B (Supplementary Table 2). Five of the samples were collected from the LC-MSA Upper, of which two (46447 and 111400) were from the upper-dune sand and three (46467, 20720 and 111401) were from the lower-dune sand (see Supplementary Information for discussion of stratigraphy details). The other four sediment samples were collected from the LC-MSA archaeological sediments: sample 111402 from the LC-MSA Middle, and samples 111403, 111404 and 20721 from the LC-MSA Lower sediments. We also collected one additional sample (111406) from the lowermost unexcavated LC-MSA sediments cemented to the south cave wall. Details of the OSL laboratory methods and results are presented in Supplementary Information.

30. Marean, C. W., Nilssen, P. J., Brown, K., Jerardino, A. & Stynder, D. Paleoanthropological investigations of Middle Stone Age sites at Pinnacle Point, Mossel Bay (South Africa): Archaeology and hominid remains from the 2000 Field Season. *Paleoanthropology* **2**, 14–83 (2004).
31. Dibble, H., Marean, C. & McPherron, S. P. The use of barcodes in excavation projects. *The SAA Archaeological Record* **7**, 33–38 (2007).
32. Geneste, J. M. *Analyse Lithique d'Industries Mousteriennes Perigord: Une Approche Technologique du Comportement des Groupes Humains au Paleolithique Moyen*. PhD thesis, Univ. of Bordeaux (1985).
33. Volman, T. P. *The Middle Stone Age in the Southern Cape*. PhD thesis, Univ. of Chicago (1981).
34. Waelbroeck, C. *et al.* Sea-level and deep water temperature changes derived from benthic foraminifera isotopic records. *Quat. Sci. Rev.* **21**, 295–305 (2002).